

## LYMPHOID NEOPLASIA

# Early-life infection depletes preleukemic cells in a mouse model of hyperdiploid B-cell acute lymphoblastic leukemia

Ali Farrokhi,<sup>1</sup> Tanmaya Atre,<sup>1</sup> Samuel Salitra,<sup>1</sup> Maryam Aletaha,<sup>1</sup> Ana Citlali Márquez,<sup>1</sup> Matthew Gynn,<sup>1</sup> Mario Fidanza,<sup>1</sup> Sumin Jo,<sup>1</sup> Nina Rolf,<sup>1</sup> Karen Simmons,<sup>2</sup> Jesus Duque-Afonso,<sup>3</sup> Michael L. Cleary,<sup>3</sup> Alix E. Seif,<sup>4</sup> Tobias Kollmann,<sup>5</sup> Soren Gantt,<sup>6</sup> and Gregor S. D. Reid<sup>1,7</sup>

<sup>1</sup>Michael Cuccione Childhood Cancer Research Program, BC Children's Hospital Research Institute, Vancouver, BC, Canada; <sup>2</sup>Division of Infectious Diseases, Department of Pediatrics, The University of British Columbia, Vancouver, BC, Canada; <sup>3</sup>Department of Pathology, School of Medicine, Stanford University, Stanford, CA; <sup>4</sup>Abramson Family Cancer Research Institute, University of Pennsylvania, Philadelphia, PA; <sup>5</sup>Department of Microbiology and Immunology, Dalhousie University, Halifax, NS, Canada; <sup>6</sup>Department of Microbiology, Infection, and Immunology, Université de Montreal, Montreal, QC, Canada; and <sup>7</sup>Division of Oncology, Hematology and Bone Marrow Transplant, Department of Pediatrics, The University of British Columbia, Vancouver, BC, Canada

## KEY POINTS

- CMV infection induces an age-dependent innate immune response mediated by STAT4- and IL-12p40, leading to PLC depletion.
- The high IFN- $\gamma$  production necessary for preleukemia depletion in neonate mice can be achieved in adult mice by impeding viral clearance.

**Epidemiological studies report opposing influences of infection on childhood B-cell acute lymphoblastic leukemia (B-ALL). Although infections in the first year of life appear to exert the largest impact on leukemia risk, the effect of early pathogen exposure on the fetal preleukemia cells (PLC) that lead to B-ALL has yet to be reported. Using cytomegalovirus (CMV) infection as a model early-life infection, we show that virus exposure within 1 week of birth induces profound depletion of transplanted E2A-PBX1 and hyperdiploid B-ALL cells in wild-type recipients and in situ-generated PLC in E $\mu$ -ret mice. The age-dependent depletion of PLC results from an elevated STAT4-mediated cytokine response in neonates, with high levels of interleukin (IL)-12p40-driven interferon (IFN)- $\gamma$  production inducing PLC death. Similar PLC depletion can be achieved in adult mice by impairing viral clearance. These findings provide mechanistic support for potential inhibitory effects of early-life infection on B-ALL progression and could inform novel therapeutic or preventive strategies.**

## Introduction

Acute lymphoblastic leukemia (ALL) is the most common subtype of childhood cancer, with 80% of cases involving B-cell precursor (BCP) cells.<sup>1</sup> The incidence of B-cell ALL (B-ALL) peaks between 3 and 5 years of age, with the hyperdiploid and ETV6-RUNX1 subtypes accounting for ~60% of cases.<sup>2</sup> For most B-ALL cases, the initiating event occurs in utero, with >70% of patients having detectable preleukemia cells (PLC) at birth.<sup>3-5</sup> Transformation to overt leukemia usually requires additional postnatally acquired mutations within the PLC population (ie, a second hit).<sup>6</sup> Notably, ALL-associated gene fusions are detectable in the blood of healthy newborns at a rate significantly higher than the subsequent incidence of the disease.<sup>7-10</sup> These findings indicate that early-arising PLC never progress to leukemia in most children, and prolonged survival of these cells is required for disease progression.

Although it was first hypothesized over a century ago that infections influence the development of acute leukemia in children, the mechanisms underlying this association remain poorly understood. Extensive epidemiological investigations have uncovered a paradox: infections can be associated with both increased and decreased risk of leukemia.<sup>11</sup> Although surrogates of infection exposure have been correlated with protection, clinically noted infections sometimes precede ALL diagnosis.<sup>12</sup> Despite these discordant observations, epidemiological studies have repeatedly identified timing as an important factor, with infection exposures in the first year of life having the greatest influence on B-ALL risk.<sup>13-20</sup>

In vivo experimental support for the causative role of immune stressors, such as delayed infection exposure and microbial dysbiosis, in leukemia progression has been reported in studies using ETV6-RUNX1 and Pax5-haploinsufficient mouse models

of B-ALL.<sup>21-25</sup> Although the specific mechanisms remain unclear, dysregulated innate immune signaling through MyD88 has recently been identified as a potential driver of leukemogenesis in Pax5<sup>+/-</sup> mice.<sup>25</sup> In contrast, using the E $\mu$ -Ret mouse model, which develops hyperdiploid B-ALL characterized by nonrandom trisomies,<sup>26</sup> we have previously demonstrated depletion of PLC in adult mice after repeated administration of toll-like receptor ligands.<sup>27</sup> In all these studies, however, immune modulation was induced after weaning, and early-life variables, such as quantitative and qualitative differences in neonatal and adult immune responses, have not been investigated.

No specific pathogen has been definitively linked to pediatric ALL, but an increasing body of evidence suggests a role for cytomegalovirus (CMV). CMV infection is a frequent infection in children and the most common congenital infection worldwide.<sup>28-30</sup> Congenital CMV infection has been linked to increased risk of childhood ALL, with a higher prevalence in Hispanic children.<sup>31</sup> It has been proposed that CMV infection during pregnancy may alter the neonatal cytokine profiles associated with the risk of childhood ALL.<sup>32</sup> However, many infants are first exposed to CMV at day care and develop only subclinical or mild infections, characteristics associated with protection from ALL in epidemiological studies.<sup>14-16,18-20</sup> Herein, we investigated the impact of timed postnatal exposure to murine CMV (MCMV) on B-ALL using the E $\mu$ -ret and E2A-PBX1 B-ALL mouse models.<sup>26,33-35</sup> Our results reveal that age-dependent antiviral immune responses directly deplete PLC through an interferon (IFN)- $\gamma$ -driven mechanism. These findings provide a mechanistic explanation for the protective effect of early-life infections and could inform future treatment and prevention strategies for B-ALL.

## Materials and methods

Methods are described here, briefly. For a detailed description, see the supplemental Material, available on the *Blood* website.

### Mice

The E $\mu$ -ret mouse model of precursor B-ALL is maintained as Ret transgene hemizygotes on a wild-type or homozygous gene-knockout BALB/c background through in-house breeding. Female and male mice were used in all experiments. All experiments were performed in accordance with the guidelines of the Canadian Council on Animal Care under a University of British Columbia Animal Care Committee-approved protocol (A19-0197).

### Leukemia transplantation

Primary E $\mu$ -ret (BALB/c) or E2A-PBX1 (C57BL/6) leukemia cells were injected into 1- to 2-day-old neonatal and 4- to 5-week-old adult mice, via the superficial temporal vein and tail vein, respectively (supplemental Figure 1). Four or 5 days after cell injection, recipient mice were infected intraperitoneally with MCMV or injected with phosphate-buffered saline. For depletion experiments, mice were euthanized 10 days post infection (dpi) for assessment of leukemia cell burden in bone marrow (BM) and spleen by flow cytometry. For survival experiments, following leukemia transplantation and MCMV infection, mice were monitored twice weekly for experimental end points,

defined by the presence of palpable lymph nodes and/or 20% weight loss.

### Virus and infection

Generally, mice were infected 1 or 4 weeks after birth. Where relevant, other time points are indicated in figure legends. Neonatal and adult mice received  $3 \times 10^3$  plaque-forming units (pfu) via intraperitoneal injection. The firefly luciferase-expressing K181-luc MCMV strain was obtained from Helen Farrell of the Queensland University.<sup>36</sup>

### Tissue processing and flow cytometry

To evaluate PLC burden, single-cell suspensions were prepared from the spleen and BM of neonatal and adult mice at 10 dpi and analyzed by flow cytometry. A list of fluorochrome-conjugated antibodies used in each staining panel is shown in supplemental Table 1. For flow cytometry-based cell sorting, PLC or leukemic cells were purified using a MoFlo Astrios EQ cell sorter (Beckman Coulter Inc) according to their phenotype (Lin<sup>-</sup> B220<sup>int</sup>/CD19<sup>+</sup>/BP-1<sup>hi</sup>).

### Cytokine neutralization and cell depletion

For cytokine neutralization and natural killer (NK) cell depletion experiments, mice received 50  $\mu$ g of antibodies via intraperitoneal injection (supplemental Table 1) at designated time points.

### RNA sequencing

PLC from MCMV-infected and control (phosphate-buffered saline-injected) E $\mu$ -ret pups were flow-sorted 7 days after treatment, and RNA was isolated from  $2 \times 10^5$  cells. Library preparation from RNA samples and sequencing was performed on Ion Chef and Ion Torrent S5 platforms (Thermo Fisher Scientific) following the manufacturer's protocol. Data processing and quality control were performed using the AmpliSeq RNA plug-in for the Ion Torrent S5. Data were normalized to reads per million. For gene set enrichment analysis (GSEA),<sup>37</sup> normalized counts were compared with the hallmark gene sets of the Molecular Signatures Database.<sup>38</sup>

### Cytokine and chemokine analysis

Cytokines and chemokines were detected in serum samples using the LEGENDplex Mouse Inflammation Panel (13-plex) and LEGENDplex Mouse Proinflammatory Chemokine Panel (13-plex) (BioLegend), according to the manufacturer's instructions. For interleukin (IL)-12p40, IL-12p75, IL-23p19, and IFN- $\gamma$  measurements, enzyme-linked immunosorbent assay kits were used, according to the manufacturer's instructions (BioLegend).

### Bioluminescence imaging

Bioluminescence imaging (BLI) was used to track luciferase-tagged MCMV in vivo. BLI was performed at different time intervals, mainly at 3, 6, and 10 dpi, and at end point before euthanizing the mice.

### Statistical methods

Numerical data are expressed as the mean  $\pm$  standard error. Statistical differences between the means of different groups were compared using unpaired nonparametric Mann-Whitney *t* tests, 1-way analysis of variance, and 2-way analysis of variance. Prism 9.0 software (GraphPad Software Inc, La Jolla, CA)

was used for all statistical analyses. Specific statistical tests, *n* values for each experiment, and the level of significance (*P* value) are listed in the figure legends.

## Results

### CMV infections in neonatal but not adult mice deplete preleukemic and leukemic cells

To directly test the impact of CMV infection at different ages on the progression of B-ALL, leukemic cells isolated from moribund adult E $\mu$ -ret mice were IV transplanted into 1- to 2-day-old (pup) and 4- to 5-week-old (adult) BALB/c recipients (supplemental Figure 1). Five to 6 days later, when similar engraftment patterns were detected in pups and adults (supplemental Figure 2), the mice were infected with MCMV and euthanized 10 dpi for assessment of leukemic cell burden. MCMV infection resulted in leukemia cell depletion in pups but not in adults (Figure 1A), leading to extended median survival in pups from 32 to 50 days (*P* = .0024; Figure 1B). In this setting, where a finite number of leukemia cells are transplanted, long-term survivors (>80 days) occurred only in the infected cohort. There was no change in adult survival (29 days for controls to 28 days for infected mice). To assess whether this age-dependent depletion was leukemia- or mouse strain-specific, we repeated the experiment using C57BL/6 pups and adults engrafted with B-ALL cells generated in E2A-PBX1 transgenic mice.<sup>35</sup> We observed the same age-dependent depletion of leukemic cells (Figure 1C).

Although transplant experiments can provide insights into the impact of infection in pups and adults bearing the same leukemic cell population, it is the in utero-generated, non-transformed PLC that are present in infants during early-life infections. We have recently shown that hyperdiploid B-ALL in E $\mu$ -ret mice arises from an aneuploid BCP population that is present at birth.<sup>26</sup> These neonatal PLC are readily identified by their B220<sup>int</sup>/CD19<sup>+</sup>/BP-1<sup>hi</sup> phenotype and are sufficient to cause disease in NSG (NOD-scid-IL2Ry<sup>null</sup>) recipient mice after a prolonged latency.<sup>26</sup> To evaluate the impact of infection on neonatal PLC, we infected cohorts of 1-, 2-, 3-, and 4-week-old E $\mu$ -ret mice with 3000 pfu MCMV. Significant depletion of PLC occurred in mice infected within the first week of life, whereas infection at 2, 3, or 4 weeks of age had no significant effect on PLC burden (Figure 1D). This age-dependent PLC depletion was also observed in F1 hybrid strains (BALB/c  $\times$  C57BL/6 and BALB/c  $\times$  FVB) carrying the E $\mu$ -ret transgene (supplemental Figure 3A), suggesting that the inherent susceptibility of the mouse strain to MCMV infection is not a determining factor.<sup>39</sup>

Titration of MCMV revealed that significant PLC depletion was also achieved in pups receiving a 10-fold lower or higher viral dose (supplemental Figure 3B). Because 3000 pfu was sufficient to induce maximal PLC depletion in neonates without causing weight loss or adverse physiological effects (supplemental Figure 3B-C), we used this dose for the remainder of this study. To evaluate whether the impact of MCMV infection was specific to the PLC population or symptomatic of a broader effect on BCPs, we quantified cell numbers in progenitor B-cell fractions (Fr<sub>s</sub>; defined using the Hardy nomenclature; supplemental Figure 4).<sup>40</sup> Although significant changes in FrA (B220<sup>+</sup>CD43<sup>+</sup>CD24<sup>+</sup>BP1<sup>-</sup>) and FrB (B220<sup>+</sup>CD43<sup>+</sup>CD24<sup>+</sup>BP1<sup>-</sup>)

were detected, these resulted from an increase in cell numbers following infection (Figure 1E). Only FrC (B220<sup>+</sup>CD43<sup>+</sup>CD24<sup>+</sup>BP1<sup>+</sup>), which contains the PLC population, was depleted by infection, showing significantly reduced numbers in both spleen and BM (Figure 1E). Despite the ongoing generation of PLC resulting from constitutive transgene expression, infected E $\mu$ -ret pups succumbed to overt disease later than uninfected controls (median age, 196 days vs 154 days; *P* = .017; Figure 1F). Collectively, these results indicate that neonatal MCMV infection systemically depletes PLC, causing a significant delay in leukemogenesis.

### PLC depletion is a by-product of the neonatal anti-MCMV immune response

To identify the mechanism mediating the decline in preleukemia burden after MCMV infection, we first analyzed the kinetics of PLC depletion in neonates. Although no depletion was observed at 6 dpi, by 10 dpi there was >90% loss of PLC from spleen and BM (Figure 2A). This timing is coincident with the transition from disseminated infection to the resolution stage, as revealed by BLI after infection with luciferase-tagged MCMV (Figure 2B), and is associated with a significant increase in spleen weight resulting from inflammatory cell infiltration (*P* < .001; supplemental Figure 5A). Despite the high viral burden before the period of PLC depletion, MCMV particles were not detected by polymerase chain reaction in PLC purified from spleens of infected pups at 7 dpi (Figure 2C). This suggests that direct viral lysis was not the primary mechanism of PLC depletion.

Neonatal and adult immune responses are quantitatively and qualitatively different, including distinct T-helper type 1 (Th1)/Th2 response skewing.<sup>41-44</sup> To investigate the contribution of Th1 and Th2 responses to PLC depletion, we infected neonatal Stat4-deficient (R/Stat4) and Stat6-deficient (R/Stat6) E $\mu$ -ret mice, which are skewed toward Th2 and Th1 cell differentiation, respectively.<sup>45</sup> Infected R/Stat6 neonates showed significant PLC depletion (*P* < .005), whereas R/Stat4 neonates exhibited no change in PLC numbers (Figure 2D). Notably, R/Stat4 neonates failed to deplete PLC despite a higher systemic viral load and delayed control of infection compared with wild-type E $\mu$ -ret pups (Figure 2E), further supporting that viral lysis is unlikely to be responsible for the PLC depletion.

Apoptosis of BM B-lineage cells has been reported after influenza and lymphocytic choriomeningitis virus infections in adult mice.<sup>46,47</sup> To determine if the loss of E $\mu$ -ret PLC after MCMV exposure was due to apoptosis, we analyzed neonatal PLC for caspase 3/7 activity at 7 dpi, a time point for which our results indicate is early in the depletion process. PLC from CMV-infected pups showed significantly higher caspase activity than those from uninfected pups (*P* = .0012; Figure 2F; supplemental Figure 5B), indicating the induction of apoptosis. These results suggest that STAT4-dependent immune effector mechanisms, rather than direct viral cytotoxicity, are responsible for the depletion of PLC observed in E $\mu$ -ret neonates.

### Depletion of PLC is dependent on IL-12/IL-23p40 but independent of IL-12 and IL-23

The requirement for STAT4 signaling suggests a role for the IL-12 family cytokines in PLC depletion. Given that IL-12 and IL-23

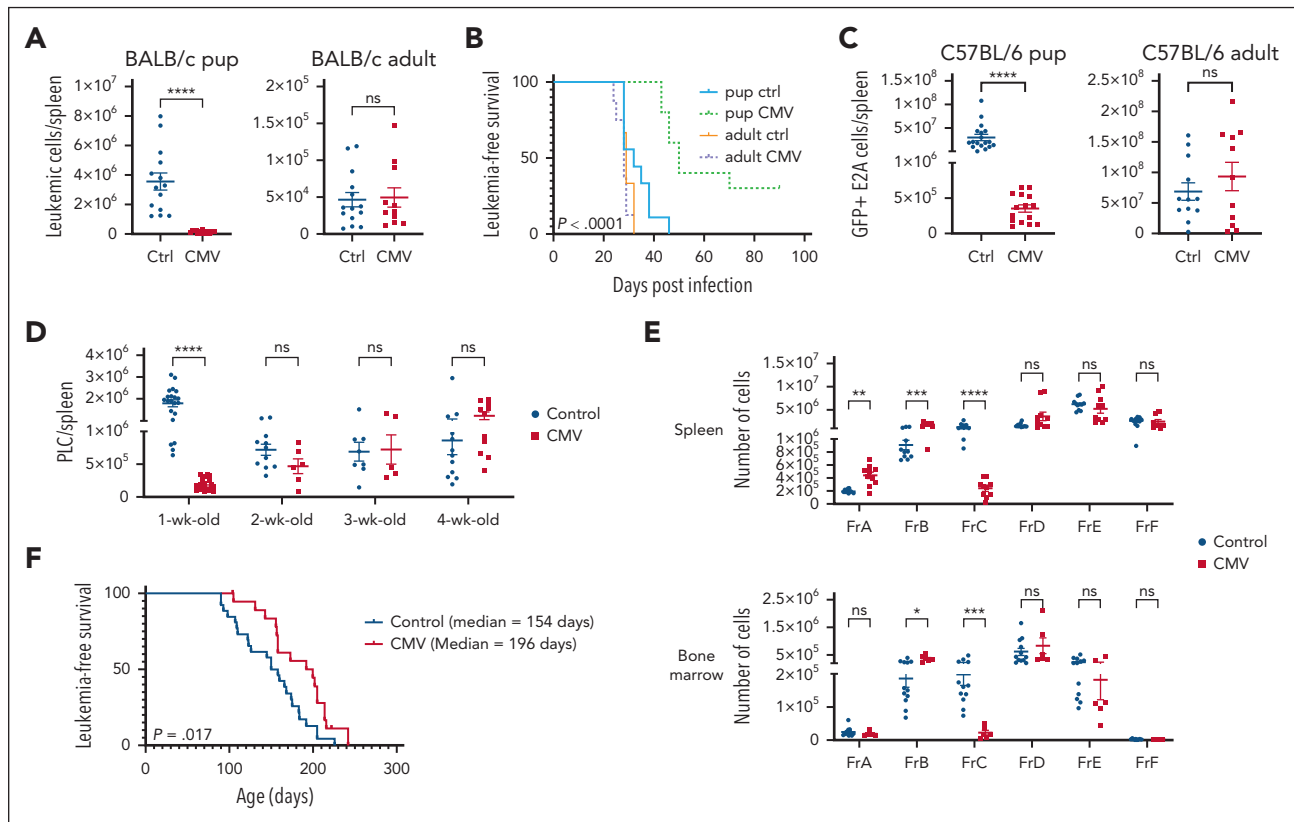


**Figure 1. Depletion of B-ALL-associated cells after timed MCMV infections.** (A) Neonatal and adult BALB/c mice injected with  $1$  to  $2 \times 10^3$  E $\mu$ -ret leukemic cells were euthanized at 10 dpi to assess leukemic cell burden in spleens of phosphate-buffered saline (PBS)-injected (control [Ctrl]) or virus-infected (CMV) recipients (Mann-Whitney;  $n = 14$  Ctrl and 16 CMV neonates;  $n = 14$  Ctrl and 11 CMV adults; pooled results for 3 different leukemias). (B) Neonatal and adult BALB/c mice injected with  $0.5$  to  $1 \times 10^3$  E $\mu$ -ret leukemic cells were infected 5 to 6 days later with PBS (Ctrl) or virus (CMV) and then monitored for leukemia-free survival of recipients (log-rank [Mantel-Cox] test;  $n = 6$ -10 mice in each group; pooled results from 2 independent experiments). (C) Neonatal and adult C57BL/6 mice injected with  $0.5$  to  $1 \times 10^3$  E2A-PBX1 leukemic cells were euthanized 10 days after subsequent infection to assess leukemic burden in spleens of PBS- or CMV-infected recipients (Mann-Whitney;  $n = 18$  Ctrl and 15 CMV-infected neonates;  $n = 12$  Ctrl and 11 infected adults; pooled results from 4 independent experiments). (D) Splenic PLC burden in E $\mu$ -ret mice 10 days after injection with PBS or CMV at the indicated age (Mann-Whitney test; number of mice in Ctrl/infected groups: week 1 [wk1] = 21/21, wk2 = 11/6, wk3 = 8/5, and wk4 = 12/11). (E) Spleen ( $n = 11$  Ctrl;  $n = 10$  CMV) and BM ( $n = 12$  Ctrl;  $n = 6$  CMV) B-cell Fr cell numbers in neonatal E $\mu$ -ret mice 10 days after injection with PBS or CMV at 5 to 7 days of age (Mann-Whitney test). (F) Leukemia-free survival of neonatal E $\mu$ -ret mice after PBS (Ctrl) or virus (CMV) injection at 5 to 7 days of age (log-rank [Mantel-Cox] test;  $n = 23$  Ctrl;  $n = 17$  CMV;  $*P = .0166$ ). All data presented as mean  $\pm$  standard error of the mean (SEM). ns, not significant;  $*P < .05$ ;  $**P < .01$ ;  $***P < .001$ ;  $****P < .0001$ . Ctrl, control.

responses differ between pups and adults,<sup>42</sup> we measured IL-12, IL-23, and IL12/IL23p40 (p40) subunit in neonatal and adult mice at 3, 6, and 10 dpi. Although neither IL-12 nor IL-23 were detected at any time point in neonates or adults, p40 revealed an age-dependent response to infection, with increased production in pups reaching a peak at 6 dpi ( $2297 \pm 280$  vs  $872 \pm 107$  pg/mL;  $P = .002$ ) and remaining elevated at 10 dpi ( $2191 \pm 307$  vs  $667 \pm 79$  pg/mL;  $P < .0001$ ; Figure 3A). To directly assess the contribution of elevated p40 production to PLC depletion activity, we administered cytokine-specific neutralizing antibodies to neonates on day 4 after infection. Consistent with the cytokine production response, neutralization of IL-12, IL-23, or both failed to block depletion; only the antibody that targets the p40 subunit prevented the depletion of PLC in infected pups (Figure 3B-C).

NK cells and CD8<sup>+</sup> T cells play a crucial role in controlling CMV primary infection and respond to IL-12 family cytokines.<sup>48-50</sup> To evaluate the potential role of T cells in PLC depletion, we generated E $\mu$ -ret mice lacking the Rag-1 gene, which still generate a PLC population despite the absence of recombinase

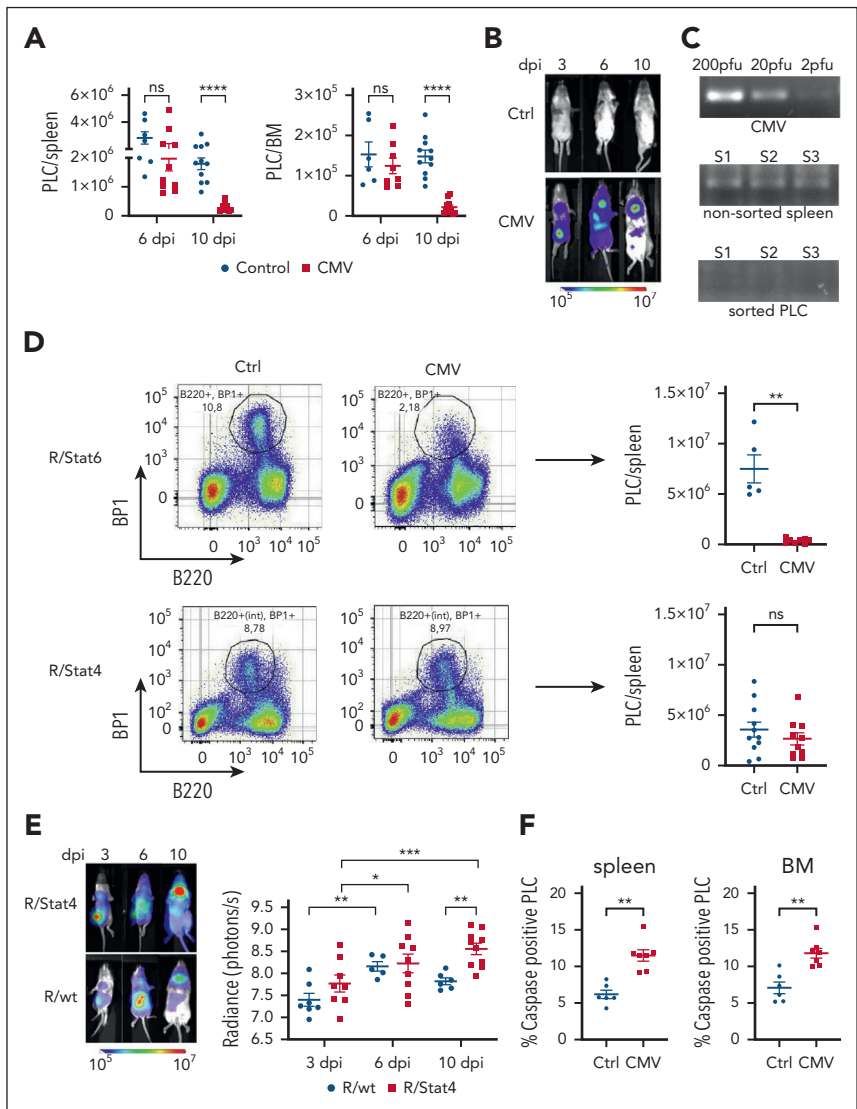
activity (supplemental Figure 6). Infection of neonatal Rag-1 gene mice efficiently depleted PLC (Figure 3D, left panel). Similarly, depletion of NK cells from E $\mu$ -ret neonates by administration of anti-asialo GM1 antibody failed to prevent PLC depletion (Figure 3D, right panel; supplemental Figure 7). These results indicate that while possibly contributing to PLC depletion in wild-type mice, neither RAG activity-dependent immune responses nor NK cells are required for the STAT4-p40-dependent reduction in PLC burden.

### PLC respond directly to infection-induced inflammatory immune responses

To identify the specific cellular changes in PLC affected by an anti-MCMV immune response and the effector molecules driving them, we analyzed gene expression in PLC from spleens of infected and noninfected E $\mu$ -ret pups at 7 dpi. Among the 23 930 genes screened, a total of 1395 differentially expressed (DE) genes were identified (fold change  $>1.5$  or below  $-1.5$ ;  $P < .05$ ), among which 629 DE genes were upregulated and 769 DE genes were downregulated. The hierarchical clustering for all DE genes and the heat map for the top 50 differentially

**Figure 2. Apoptosis of PLC after MCMV infection is STAT4-dependent.**

(A) Comparison of PLC numbers in spleen (left) and BM (right) of PBS- (blue) or CMV-injected (red) 1-week-old E $\mu$ -ret pups at 6 and 10 dpi (Mann-Whitney t test;  $n = 7$  PBS and 10 CMV neonates; pooled results from 3 independent experiments). (B) Representative images of bioluminescence in 1-week-old E $\mu$ -ret pups infected with luciferase-tagged CMV and uninfected controls at 3, 6, and 10 dpi. (C) Polymerase chain reaction for detecting CMV DNA in 3 different concentrations of virus equal to 200, 20, and 2 pfu as controls, 3 unsorted total splenocytes, and 3 sorted PLC samples from spleens of wild-type E $\mu$ -ret pups 7 days after infection from 3 independent experiments. (D) Comparison of PLC numbers in representative (left panels) or cumulative (right panels) spleens of PBS- or CMV-injected Stat4 $^{-/-}$  (R/Stat4) and Stat6 $^{-/-}$  (R/Stat6) E $\mu$ -ret pups at 10 dpi (Mann-Whitney test; R/Stat4,  $n = 11$  PBS and 10 CMV; R/Stat6,  $n = 5$  PBS and 8 CMV; pooled results from 3 independent experiments). (E) Representative (left panel) or cumulative (right panel) bioluminescence in wild-type (R/wt) and Stat4 $^{-/-}$  (R/Stat4) E $\mu$ -ret pups at 3, 6, and 10 dpi with luciferase-tagged CMV (2-way analysis of variance [ANOVA];  $n = 5-10$ ) (for simplicity, nonsignificant comparisons are not labeled). (F) Cumulative results for assessment of caspase 3/7 activity in PLC (CD19 $^{+}$ , BP1 $^{+}$ ) from spleen and BM of E $\mu$ -ret pups 7 days after PBS (Ctrl) or virus (CMV) injection (Mann-Whitney t test; PBS,  $n = 6$ ; MCMV,  $n = 7$ ). Data shown as mean  $\pm$  SEM. ns, not significant; \* $P < .05$ ; \*\* $P < .01$ ; \*\*\* $P < .001$ ; \*\*\*\* $P < .0001$ .



upregulated and downregulated genes are shown in supplemental Figure 8A-B.

GSEA was performed to explore the differences in transcriptional profiles after infection. Of the 50 hallmark gene sets, 21 were upregulated (11 at a false discovery rate [FDR] <25%) and 29 were downregulated (14 at FDR <25%) in PLC from infected pups. IFN- $\alpha$ , IFN- $\gamma$ , tumor necrosis factor- $\alpha$  (TNF- $\alpha$ ), and inflammatory pathways were among the most significantly upregulated gene sets (Figure 4A-B), whereas gene sets related to cell cycle control and metabolism were among the downregulated pathways (Figure 4C-D; supplemental Figure 8C). To validate the RNA sequencing findings, we used flow cytometry to confirm the changes in expression of several cell surface molecules, including CD40, PD-L1, Sca-1, and CD86, that showed elevated expression after infection (supplemental Figure 8D). In addition, gene sets related to apoptosis were also among the upregulated pathways in GSEA of CMV-exposed PLC based on hallmark gene sets (FDR <25%, but  $P = .14$ ). This was consistent with the initiation of PLC apoptosis detected by flow cytometry at the same early time point

(Figure 2F). These results confirmed that changes in the immune environment induced by MCMV infection directly affect the neonatal PLC population.

**IFN- $\gamma$  is the driver of PLC depletion in neonates after MCMV infection**

The gene expression changes in PLC from infected neonates indicate exposure to inflammatory cytokines, particularly IFN- $\alpha$ , IFN- $\gamma$ , and TNF- $\alpha$ . To determine whether differences in the inflammatory response between neonatal and adult mice could account for their contrasting effects on preleukemia, we measured proinflammatory and inflammatory chemokines and cytokines in the sera of pups and adults at 3, 6, and 10 dpi. Fifteen of the 25 chemokines and cytokines analyzed showed increased levels in infected pups, with most peaking at 6 dpi (Figure 5A-B). In adults, only CXCL9 achieved significantly elevated expression at 10 dpi ( $P = .01$ ); IFN- $\gamma$  and TNF- $\alpha$  showed slightly, but not significantly, enhanced expression ( $P > .1$ ). We did not detect any changes in the levels of LIX (CXCL15), macrophage inflammatory protein 3 $\alpha$  (CCL20), TARC (CCL17),

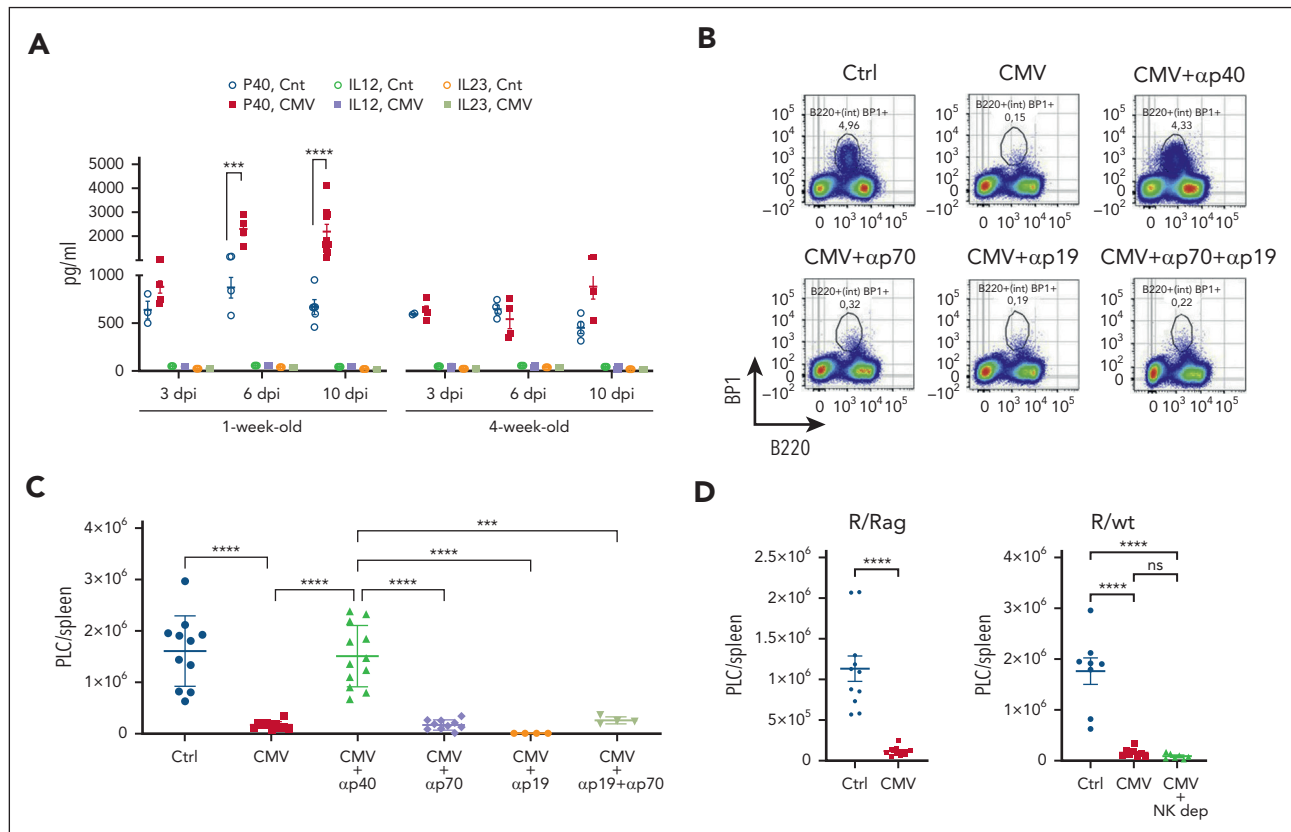


**Figure 3. Depletion of PLC is dependent on IL-12p40.** (A) Enzyme-linked immunosorbent assay (ELISA)-based quantification of IL-12p40 (anti-p40 antibody [Ab]), IL-12 (anti-p70 Ab), and IL-23 (anti-p19 Ab) in sera from neonate and adult E $\mu$ -ret mice at 3, 6, and 10 dpi (Mann-Whitney;  $n = 3-7$ ). (B) Representative flow cytometry plots showing PLC in splenocytes of E $\mu$ -ret pups after CMV infection in the presence of indicated neutralizing antibodies. (C) Cumulative results showing PLC burden in spleens of E $\mu$ -ret pups infected along with p40, p19, and/or p70 neutralizing antibodies (1-way ANOVA;  $n = 4-11$ ). (D) PLC numbers in spleens of PBS (Ctrl) or virus (CMV)-injected Rag1<sup>-/-</sup> (R/Rag, left panel), wild-type (R/wt), and NK-depleted wt (NK-dep, right panel) E $\mu$ -ret pups at 10 dpi (Mann-Whitney; R/Rag1,  $n = 10$  PBS and 10 MCMV; 1-way ANOVA;  $n = 8$  PBS, 8 CMV, and 7 CMV + NK-depleted; pooled results from 3 independent experiments). All data presented as mean  $\pm$  SEM (\*\*\* $P < .001$ ; \*\*\*\* $P < .0001$ ). ns, not significant (nonsignificant comparisons in graphs A and C are not labeled).

MDC (CCL22), IL-23, IL-10, IL-1 $\beta$ , IL-12p70, IL-17, or IL-27 in neonates and adults at any time point (data not shown). These results indicate a distinct inflammatory immune response in neonates during the PLC depletion process.

Given the robust PLC response signatures to the highly up-regulated cytokines IFN- $\gamma$  and TNF- $\alpha$ , we next tested the impact of antibody-mediated neutralization of these cytokines, as well as chemokines CCL2 and CXCL9. As expected, the viral load in IFN- $\gamma$ - and TNF- $\alpha$ -neutralized pups was higher than in the infected control group, emphasizing their role in the immune response against MCMV (Figure 5C). Despite this higher viral load, neutralizing IFN- $\gamma$  in CMV-infected pups completely blocked PLC depletion (Figure 5D), whereas TNF- $\alpha$  neutralization achieved only partial inhibition with no significant difference relative to controls ( $P = .4602$ ) or CMV-infected ( $P = .5395$ ) mice. Despite having a clear impact on the proinflammatory response (supplemental Figure 9), neutralization of either CCL2 or CXCL9 did not prevent PLC depletion (Figure 5D), indicating that not all inflammatory mediators upregulated after viral infection impact the preleukemia burden. This result demonstrates a primary role for IFN- $\gamma$  and confirms that it is the response to the virus, and not the virus itself, that leads to PLC depletion.

To understand the interactions between STAT4, IL-12p40, and IFN- $\gamma$ , we measured the levels of proinflammatory/inflammatory chemokines and cytokines at 6 dpi in sera from E $\mu$ -ret and R/Stat4 pups and from IL-12p40-neutralized and IFN- $\gamma$ -neutralized E $\mu$ -ret pups. IFN- $\gamma$  production was significantly reduced in infected R/Stat4 and IL-12p40-neutralized pups, whereas IFN- $\gamma$  neutralization had no effect on IL-12p40 levels (Figure 5E). The broader impact of these specific immune deficiencies and manipulations on the complete inflammatory response is shown in supplemental Figure 10.

These results indicated that IFN- $\gamma$  is a late contributor to PLC depletion. To evaluate the contribution of IFN- $\gamma$  alone, we exposed in vitro cocultures of PLC with stromal cells to 1-ng/mL IFN- $\gamma$ . Significant inhibition of PLC expansion was observed in the presence of IFN- $\gamma$  (Figure 6A). Although concentrations  $>5$  ng/mL had a detrimental effect on both stromal cells and PLC, 1 and 0.5 ng/mL selectively depleted the PLC without any adverse effect on stromal cells (supplemental Figure 11). To confirm that IFN- $\gamma$  alone was sufficient to drive PLC depletion in vivo, we injected IFN- $\gamma$  into E $\mu$ -ret pups. Injection of as little as 1- $\mu$ g IFN- $\gamma$  every other day for 7 days resulted in a significant depletion of splenic PLC (Figure 6B). Consistent with its role as a final effector molecule downstream of STAT4, injection of

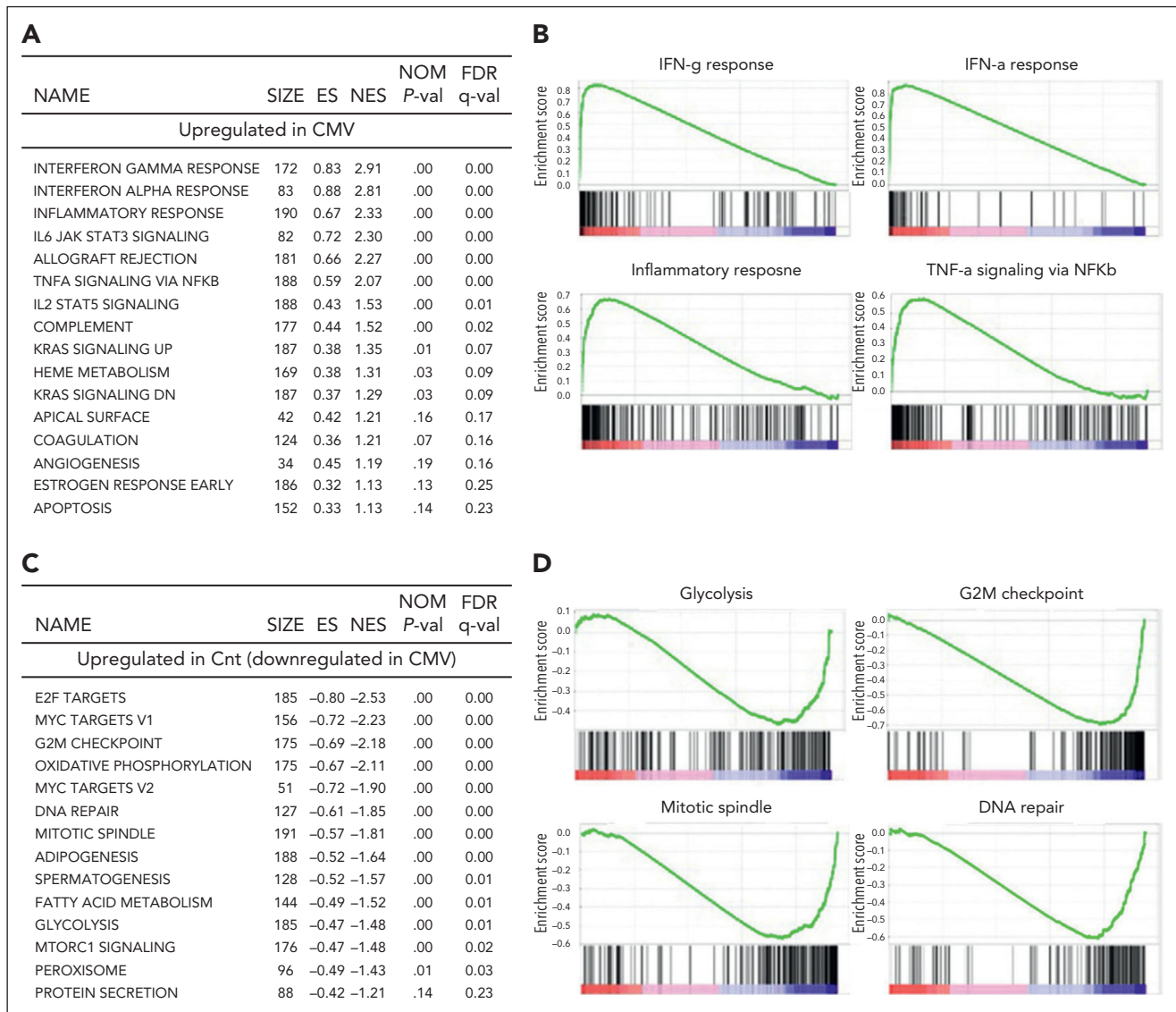


**Figure 4. Gene expression analysis indicates pathway utilization changes in PLC after neonatal MCMV infection.** Selected gene sets from the Molecular Signatures Database, Molecular Hallmarks (hallmark gene sets) collection, enriched among upregulated and downregulated pathways in PLC from MCMV-infected neonates compared with PBS-injected controls (ranked according to decreasing normalized enrichment score). (A) Top 16 statistically significant upregulated biological pathways. (B) GSEA enrichment plots showing upregulation of gene sets representing IFN- $\alpha$ , IFN- $\gamma$ , and TNF- $\alpha$ , and inflammatory responses. (C) Top 14 downregulated biological pathways. (D) GSEA enrichment plots showing downregulation of gene sets representing cell cycle and metabolism. ES, enrichment score; FDR, false discovery rate; NES, normalized enrichment score; NOM, nominal; size, number of genes in each set.

exogenous IFN- $\gamma$  into R/Stat4 pups showed a profound depletion of PLC (Figure 6C). Further, exogenous IFN- $\gamma$  alone was sufficient to fully replicate the pattern of BCP Fr-specific changes induced by neonatal MCMV infection (Figure 6D).

### Impaired viral clearance generates a PLC-depleting immune response in adult mice

Consistent with the reduced antiviral protection in neonates, the highest systemic burden of MCMV was detected in pups infected at 1 week of age (supplemental Figure 12A). Mice infected at 2, 3, and 4 weeks of age showed progressively improved control of the virus. Notably, lower-efficiency virus control was associated with higher levels of IFN- $\gamma$  production, most notably at 6 dpi (supplemental Figure 12B). To investigate if impaired control of MCMV in older mice would similarly

generate high IFN- $\gamma$  levels and, as a result, deplete PLC, we made use of the fact that NK cells are not required for PLC depletion (Figure 3D) but play a prominent role in defense against MCMV. As expected, depletion of NK cells from 4-week-old  $\epsilon\mu$ -ret mice significantly delayed control of MCMV infection, as indicated by higher bioluminescence at 3, 6, and 10 dpi (Figure 7A; supplemental Figure 13), and this was associated with significantly higher serum levels of IL-12p40 and IFN- $\gamma$  (Figure 7B). Notably, this altered immune response to MCMV achieved significant PLC depletion (Figure 7C). To confirm that elevated IFN- $\gamma$  was sufficient to achieve PLC depletion in older mice, we injected 4-week-old  $\epsilon\mu$ -ret mice with IFN- $\gamma$ . Consistent with the result observed in similarly treated pups (Figure 6D), exogenous IFN- $\gamma$  induced a profound depletion of the BCP Fr-containing PLC in both BM and spleen (Figure 7D).

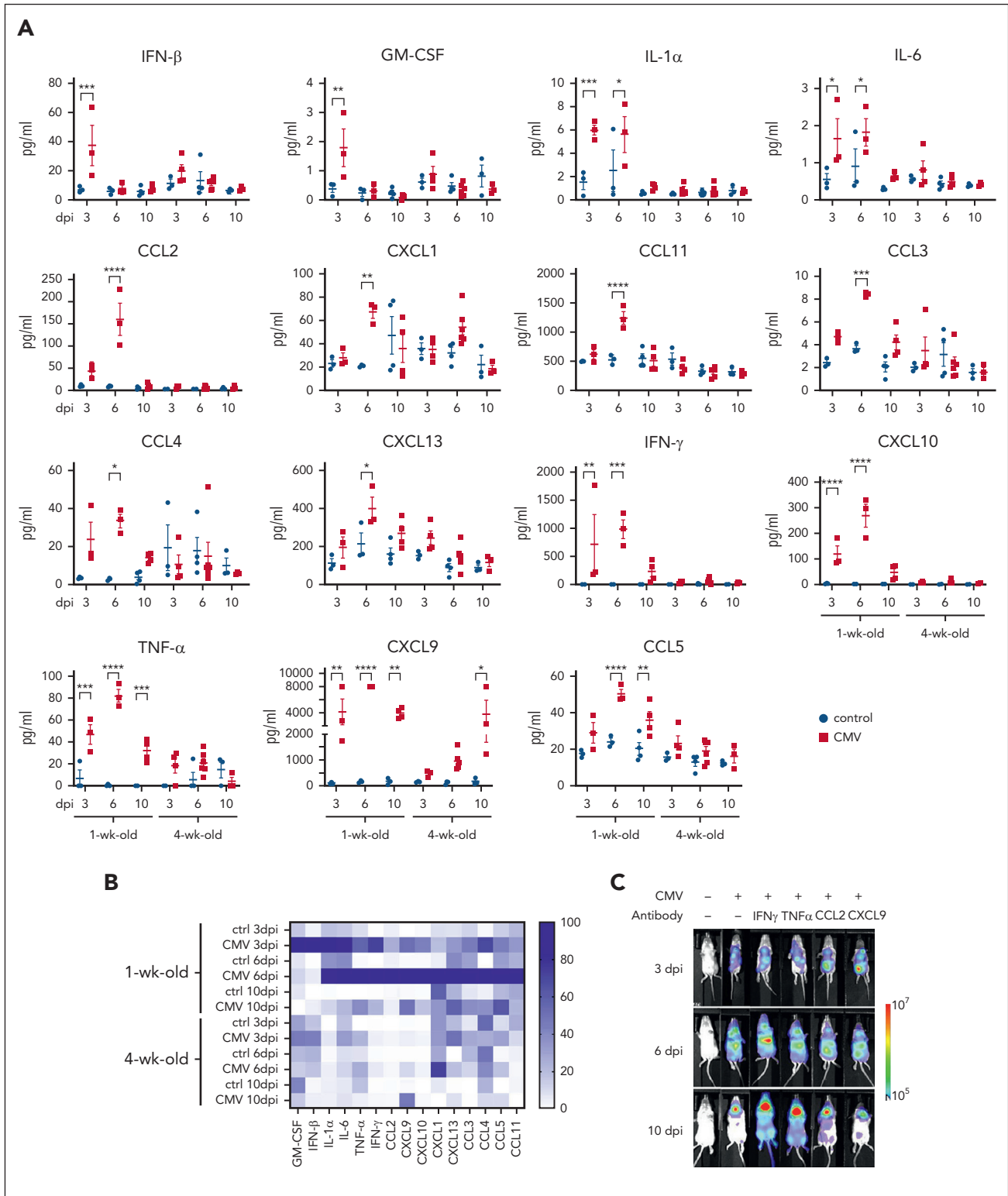


**Figure 5. Inflammatory responses following MCMV infection of neonatal and adult E $\mu$ -ret mice.** (A) Flow cytometry–based quantification of 15 proinflammatory/inflammatory cytokines and chemokines that were significantly higher in the serum of MCMV-infected pups (1-week-old) compared with adult (4-week-old) E $\mu$ -ret mice at 3, 6, or 10 dpi (2-way ANOVA; comparison between PBS-injected [Ctrl] and infected [CMV] conditions within each group have been shown; n = 3-5). (B) Heat map depicting the inflammatory response. Normalized means (averaged from 3-5 samples per group) calculated for each cytokine by taking smallest mean as 0% and largest mean as 100%. (C) Representative bioluminescence images of E $\mu$ -ret pups at 3, 6, and 10 days after infection with luciferase-tagged MCMV in the presence of the indicated neutralizing antibodies. (D) PLC burden in the spleen of PBS (Ctrl) and virus (MCMV)-infected E $\mu$ -ret pups also injected with the indicated neutralizing antibodies (1-way ANOVA; n = 3-5). (E) ELISA-based quantification of p40 and flow cytometry–based quantification of IFN- $\gamma$ , and TNF- $\alpha$  in sera from control and MCMV-infected wild-type (R/wt), Stat4<sup>-/-</sup> (R/Stat4), IFN- $\gamma$ -neutralized, and p40-neutralized E $\mu$ -ret mice at 6 dpi (2-way ANOVA; followed by Tukey test; n = 3-4). For the simplicity of graphs, comparisons between MCMV-infected groups are shown. All data are presented as mean  $\pm$  SEM. \*P < .05; \*\*P < .01; \*\*\*P < .001; \*\*\*\*P < .0001 (nonsignificant comparisons are not labeled).

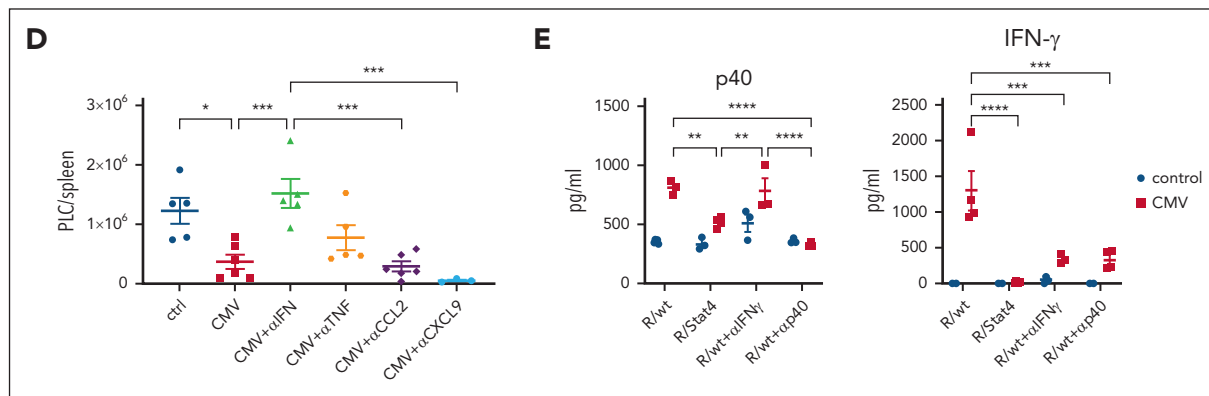
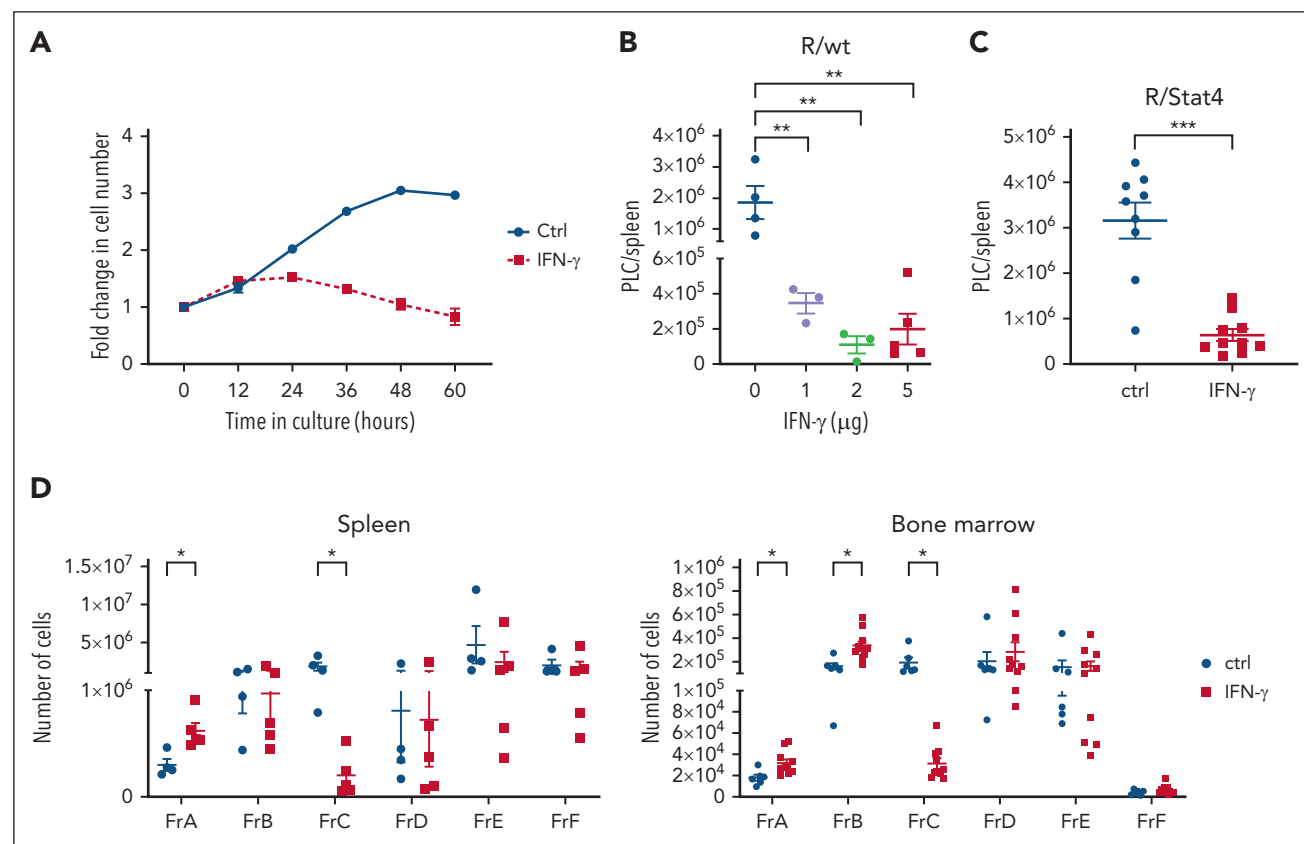


Figure 5 (continued)

## Discussion

In most cases of B-ALL, leukemia onset results from secondary genetic lesions occurring in preleukemic BCPs that are generated in utero. Despite this, to date, there have been no studies on the direct impact of early-life virus exposure on fetal PLC. To our knowledge, the findings presented herein provide the first evidence that PLC respond directly to changes in the early-life immune environment induced by infection, showing

alterations in cell surface phenotype, intracellular pathway utilization, and survival. In the presence of high levels of IFN- $\gamma$ , these changes result in a significant reduction in PLC burden, but only when virus exposure occurs within 7 days of birth. Depletion is restricted to PLC/FrC cells and does not reflect a general impact on B-lineage cells. The same age-dependent pattern of depletion is observed in C57BL/6 and BALB/c mice bearing transplanted leukemic cells, indicating that the



**Figure 6. Exogenous IFN- $\gamma$  replicates BCP Fr-specific depletion of PLC.** (A) Change in cell number of flow-sorted PLC cocultured on stromal cells in the absence (Ctrl) or presence (IFN- $\gamma$ ) of 1-ng/mL IFN- $\gamma$  for 60 hours. Quantification of PLC was achieved by Incucyte (Sartorius) live-cell analysis at 6-hour intervals. (B) PLC burden in the spleens of noninfected wild-type (R/wt) E $\mu$ -ret pups after administration of different concentrations of IFN- $\gamma$  (1, 2, or 5  $\mu$ g/dose) every 2 days, from 9 to 16 days of age (1-way ANOVA;  $n = 3-5$ ;  $**P < .005$ ). (C) PLC burden in spleens of noninfected Stat4 $^{-/-}$  (R/Stat4) E $\mu$ -ret mice injected with 5  $\mu$ g/dose IFN- $\gamma$  every 2 days, from 9 to 16 days of age (Mann-Whitney test;  $n = 9-10$ ;  $***P < .005$ ). (D) Spleen (left panel) and BM (right panel) B-cell Fr burden in PBS (Ctrl) and 5  $\mu$ g/dose IFN- $\gamma$ -injected neonatal E $\mu$ -ret mice (Mann-Whitney test; spleen:  $n = 4$  Ctrl and 5 IFN- $\gamma$ ; and BM  $n = 6$  Ctrl and 10 IFN- $\gamma$ ;  $*P < .05$ ). All data are presented as mean  $\pm$  SEM. Nonsignificant comparisons in all graphs are not labeled.

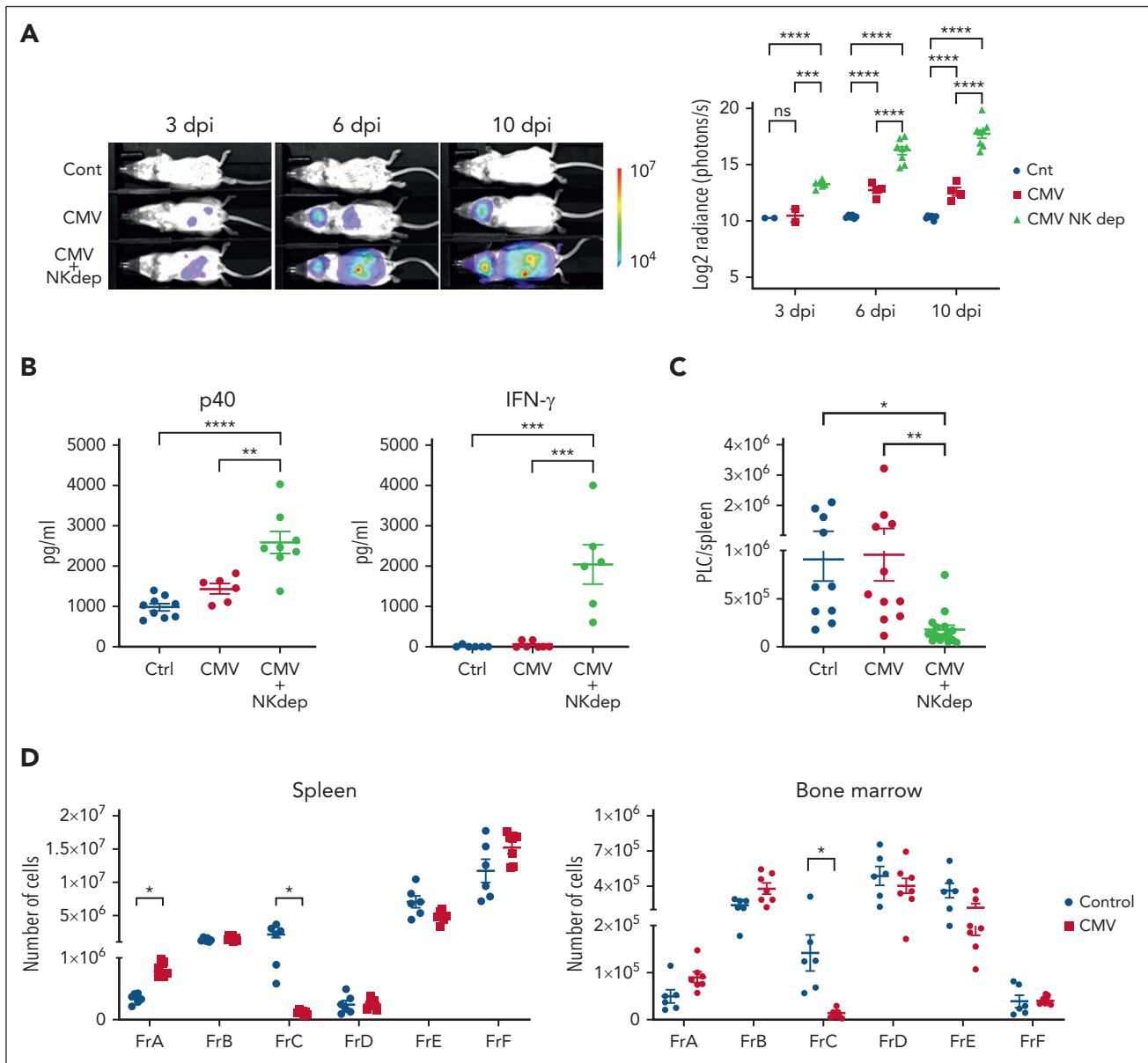


**Figure 7. Impaired viral clearance generates a PLC-depleting IFN- $\gamma$ -mediated immune response in adult mice.** (A) Representative images and overall plot of bioluminescence in 4-week-old E $\mu$ -ret pups infected with luciferase-tagged CMV with and without NK cell depletion (and uninfected controls) at 3, 6, and 10 dpi. For NK cell depletion, 50- $\mu$ g asialo GM1 antibody was administered at days -3, -1, +1, +4, and +7 (day 0 was the time of infection) (2-way ANOVA;  $n = 4-8$ ; \*\*\*\* $P < .0001$ ). (B) ELISA-based quantification of IL-12p40 (anti-p40 Ab) and IFN- $\gamma$  (anti-IFN- $\gamma$  Ab) in sera from PBS-injected control and CMV-infected (with and without NK depletion) adult E $\mu$ -ret mice at 10 dpi (1-way ANOVA;  $n = 6-10$ ; \*\* $P < .05$ ; \*\*\*\* $P < .0001$ ). (C) PLC burden in the spleens of PBS-injected control and CMV-infected (with and without NK depletion) adult E $\mu$ -ret mice at 10 dpi (1-way ANOVA;  $n = 10-16$ ; \* $P < .05$ ; \*\* $P < .005$ ). (D) Spleen (left panel) and BM (right panel) B-cell Fr burden after daily administration of PBS (Ctrl) or 10  $\mu$ g/dose IFN- $\gamma$  to 4-week-old adult E $\mu$ -ret mice for 7 days (Mann-Whitney test;  $n = 6$  Ctrl and 7 IFN- $\gamma$ ; \* $P < .005$ ). All data are presented as mean  $\pm$  SEM. Nonsignificant comparisons in all graphs are not labeled.

maturation stage of the responding immune system, rather than the age of the B-ALL cells, remains a primary determinant of outcome across strains with diverse immunological backgrounds.

The induction of age-restricted, PLC-depleting immune activity highlights the importance of timing of infection for protection from leukemia, as has been observed in epidemiological studies. Differences between the neonatal and adult immune systems render neonates more vulnerable to infectious agents.<sup>51-53</sup> This vulnerability was reflected in our study by the

delayed control and higher viral load observed in MCMV-infected neonates. However, MCMV itself does not directly induce PLC loss; rather, the magnitude of cytokine production in response to infection is the age-dependent variable affecting the outcome. Although there is precedent for cytokine-mediated depletion of B-lineage cells following viral infections,<sup>46,47</sup> the narrow age restriction suggests that PLC depletion is likely the result of a distinct, developmentally regulated immune response. The BCP Fr-restricted depletion pattern could be replicated by injection of exogenous IFN- $\gamma$  into 1-week or 4-week-old mice, demonstrating the primary role

of this inflammatory cytokine, which is present at significantly higher levels in the peripheral blood of infected neonates and NK cell-depleted adults. Although IFN- $\gamma$  has not been associated with ALL progression risk in studies of neonatal blood,<sup>54,55</sup> polymorphisms influencing IFN- $\gamma$  expression levels have been associated with age at clinical onset and risk groups in children with B-ALL.<sup>56</sup> Further, the prominent role of IFN- $\gamma$  in early-life depletion of PLC is consistent with our previous observations that the cytokine is a significant modifier of preleukemia burden in mouse models.<sup>27,57</sup>

Consistent with the absence of mature adaptive immunity in neonates, RAG1-dependent immune activity was not required to reduce preleukemia burden. This finding implicated a STAT4-dependent innate immune response in the depletion of PLC. STAT4 is required for IFN- $\gamma$  production by various innate immune cells, including dendritic cells, innate lymphoid cells (ILC1 and ILC3), and alveolar macrophages.<sup>58-60</sup> However, the role of the IL-12p40 subunit, rather than IL-12p70, in STAT4-dependent PLC depletion was unexpected. Similar to a classical IL-12p70-driven immune response, IL-12p40 stimulated significant production of IFN- $\gamma$  in neonates, consistent with the suggestion that IL-12p40 is an early, T cell-independent innate immune response to pathogens.<sup>61</sup> A role of IL-12p40 in protecting against ALL is consistent with the reported increased risk of ALL in premature infants and in children infected with CMV in utero,<sup>31,62</sup> 2 settings where IL-12p40 expression is largely lacking.<sup>63,64</sup>

The protective mechanisms identified in our study are in contrast to the causative role of infection that has been reported from in vivo studies using the ETV6-RUNX1 and Pax5-haploinsufficient mouse models of B-ALL.<sup>21-24</sup> In both of these models, exposure to non-SPF (specific pathogen free) housing conditions is necessary for B-ALL onset in 10% to 20% of mice, beginning at ~6 months of age. However, disruption of the microbiome by antibiotics also causes leukemia in the Pax5 model,<sup>25</sup> but not in ETV6-RUNX1 mice, suggesting that the impact of early-life variables on disease progression may not be shared across all B-ALL subtypes. Intriguingly, innate immune signaling has been implicated in both the early-life protection observed in our study, performed entirely in an SPF environment, and in the progression of B-ALL in Pax5<sup>+/-</sup> mice.<sup>25</sup> This may simply underline the importance of timing as a variable influencing the outcome. However, given that both pro- and anti-ALL activities have been attributed to purified pathogen recognition receptor ligands,<sup>25,27,65</sup> the pattern of response pathway stimulation by specific infectious agents may also be a significant variable. Furthermore, the leukemia cell of origin may also influence the outcome of infection exposure. Although ETV6-RUNX1 ALL is generally thought to arise from an abnormal hematopoietic stem cell,<sup>66,67</sup> for both hyperdiploid and E2A-PBX ALL modeled in our study, the cell of origin in most cases appears to be a lineage-committed precursor.<sup>4,68,69</sup> Defining the sensitivity of specific leukemia precursor populations to changes in their immune environment may be critical to understanding the role that infections play in the progression of each B-ALL subtype.

Surrogates for infection, including day care attendance, have been associated with reduced ALL risk, with pathogen exposure during early life appearing to be more protective than exposure later in childhood.<sup>18-20</sup> Although these findings have been

interpreted in the context of immune maturation,<sup>70,71</sup> our results reveal an alternative, or perhaps additional, protective activity that could account for the lower incidence of childhood leukemia compared with the higher frequency of ALL-associated translocations detected in newborns.<sup>7,10</sup> The profound depletion of PLC observed in neonatal mice after low-dose infection with CMV, a common cause of mild or asymptomatic illness in infants attending day care, provides a potential mechanistic explanation for the reduced ALL risk and could provide the foundation for future treatment or prevention strategies for B-ALL.

## Acknowledgments

The authors thank Amawaz Bashir, Zahra Faghih, and Zahra Savoji for excellent technical assistance; Amanda Lorentzian and Jenna Revers for assistance with RNA sequencing; and C. James Lim and Pascal Leclair for support with live-cell imaging.

This work was supported by operating grants from the Canadian Institutes of Health Research (MOP-126122 [G.S.D.R.]). A.F. was the recipient of a Michael Cuccione Childhood Cancer Research Program (MC3RP) Postdoctoral Scholarship. T.A. was the recipient of a MC3RP Research Doctoral Scholarship and the BC Children's Hospital Graduate Studentship.

## Authorship

Contribution: A.F. and G.S.D.R. conceived and designed the project, analyzed and interpreted the data (statistical analysis, biostatistics, and computational analysis), and prepared the manuscript; A.F., T.A., S.S., M.A., A.C.M., M.G., M.F., S.J., K.S., J.D.-A., and M.L.C. developed the methodology; N.R., A.E.S., T.K., and S.G. contributed intellectual, technical, or material support; and G.S.D.R. supervised the study.

Conflict-of-interest disclosure: S.G. received research funding from Moderna, Merck, VBI, Pfizer, GSK, Altona Diagnostics, and Meridian Biosciences; and consulting fees from Moderna, Merck, GSK, and Cur-evo. The remaining authors declare no competing financial interests.

ORCID profiles: A.F., 0000-0002-6345-5585; T.A., 0000-0001-9863-691X; S.S., 0000-0003-3389-228X; S.J., 0000-0003-1445-9392; N.R., 0000-0002-4531-2994; J.D.-A., 0000-0002-8287-5673; A.E.S., 0000-0002-1799-2582; T.K., 0000-0003-2403-9762; G.S.D.R., 0000-0002-7567-3424.

Correspondence: Gregor S. D. Reid, BC Children's Hospital Research Institute, Room 3084 950 West 28th Ave, Vancouver, BC V5Z 4H4, Canada; email: [gregor.reid@ubc.ca](mailto:gregor.reid@ubc.ca).

## Footnotes

Submitted 19 April 2024; accepted 29 May 2024; prepublished online on *Blood* First Edition 14 June 2024. <https://doi.org/10.1182/blood.2024025038>.

The RNA sequencing data are available in the Gene Expression Omnibus database (accession number GSE269131).

All data relevant to this study is provided in the manuscript. Requests for further information should be directed to the corresponding author, Gregor S. D. Reid ([gregor.reid@ubc.ca](mailto:gregor.reid@ubc.ca)).

The online version of this article contains a data supplement.

There is a [Blood Commentary](#) on this article in this issue.

The publication costs of this article were defrayed in part by page charge payment. Therefore, and solely to indicate this fact, this article is hereby marked "advertisement" in accordance with 18 USC section 1734.

## REFERENCES

- Hunger SP, Mullighan CG. Acute lymphoblastic leukemia in children. *N Engl J Med*. 2015;373(16):1541-1552.
- Lee SHR, Li Z, Tai ST, Oh BLZ, Yeoh AEJ. Genetic alterations in childhood acute lymphoblastic leukemia: interactions with clinical features and treatment response. *Cancers*. 2021;13(16):4068.
- Wiemels JL, Cazzaniga G, Daniotti M, et al. Prenatal origin of acute lymphoblastic leukaemia in children. *Lancet*. 1999; 354(9189):1499-1503.
- Rüchel N, Jepsen VH, Hein D, Fischer U, Borkhardt A, Gössling KL. In utero development and immunosurveillance of B cell acute lymphoblastic leukemia. *Curr Treat Options Oncol*. 2022;23(4):543-561.
- Hein D, Borkhardt A, Fischer U. Insights into the prenatal origin of childhood acute lymphoblastic leukemia. *Cancer Metastasis Rev*. 2020;39(1):161-171.
- Greaves M. A causal mechanism for childhood acute lymphoblastic leukaemia. *Nat Rev Cancer*. 2018;18(8):471-484.
- Mori H, Colman SM, Xiao Z, et al. Chromosome translocations and covert leukemic clones are generated during normal fetal development. *Proc Natl Acad Sci U S A*. 2002;99(12):8242-8247.
- Greaves M, Colman SM, Kearney L, Ford AM. Fusion genes in cord blood. *Blood*. 2011; 117(1):369-371.
- Škorvaga M, Nikitina E, Kubeš M, et al. Incidence of common preleukemic gene fusions in umbilical cord blood in Slovak population. *PLoS One*. 2014;9(3):e91116.
- Schäfer D, Olsen M, Lähnemann D, et al. Five percent of healthy newborns have an ETV6-RUNX1 fusion as revealed by DNA-based GIPFEL screening. *Blood*. 2018;131(7): 821-826.
- Hwee J, Tait C, Sung L, Kwong JC, Sutradhar R, Pole JD. A systematic review and meta-analysis of the association between childhood infections and the risk of childhood acute lymphoblastic leukaemia. *Br J Cancer*. 2017;118(1):127-137.
- Zimmermannova O, Zaliova M, Moorman AV, et al. Acute lymphoblastic leukemia with aleukemic prodrome: preleukemic dynamics and possible mechanisms of immunosurveillance. *Haematologica*. 2017; 102(6):e225-e228.
- Chan LC, Lam TH, Li CK, et al. Is the timing of exposure to infection a major determinant of acute lymphoblastic leukaemia in Hong Kong? *Paediatr Perinat Epidemiol*. 2002; 16(2):154-165.
- Ajrouch R, Rudant J, Orsi L, et al. Childhood acute lymphoblastic leukaemia and indicators of early immune stimulation: the Estelle study (SFCE). *Br J Cancer*. 2015;112(6):1017-1026.
- Rudant J, Orsi L, Menegaux F, et al. Childhood acute leukemia, early common infections, and allergy: the ESCALE study. *Am J Epidemiol*. 2010;172(9):1015-1027.
- Urayama KY, Ma X, Selvin S, et al. Early life exposure to infections and risk of childhood acute lymphoblastic leukemia. *Int J Cancer*. 2011;128(7):1632-1643.
- Morimoto LM, Kwan ML, Deosaransingh K, et al. History of early childhood infections and acute lymphoblastic leukemia risk among children in a US integrated health-care system. *Am J Epidemiol*. 2020;189(10): 1076-1085.
- Ma X, Buffler PA, Wiemels JL, et al. Ethnic difference in daycare attendance, early infections, and risk of childhood acute lymphoblastic leukemia. *Cancer Epidemiol Biomarkers Prev*. 2005;14(8):1928-1934.
- Jourdan-Da Silva N, Perel Y, Méchinaud F, et al. Infectious diseases in the first year of life, perinatal characteristics and childhood acute leukaemia. *Br J Cancer*. 2004;90(1): 139-145.
- Urayama KY, Buffler PA, Gallagher ER, Ayoob JM, Ma X. A meta-analysis of the association between day-care attendance and childhood acute lymphoblastic leukaemia. *Int J Epidemiol*. 2010;39(3): 718-732.
- Rodríguez-Hernández G, Hauer J, Martín-Lorenzo A, et al. Infection exposure promotes ETV6-RUNX1 precursor B-cell leukemia via impaired H3K4 demethylases. *Cancer Res*. 2017;77(16):4365-4377.
- Rodríguez-Hernández G, Opitz F V, Delgado P, et al. Infectious stimuli promote malignant B-cell acute lymphoblastic leukemia in the absence of AID. *Nat Commun*. 2019;10(1):5563.
- Vicente-Duenas C, Janssen S, Oldenburg M, et al. An intact gut microbiome protects genetically predisposed mice against leukemia. *Blood*. 2020;136(18):2003-2017.
- Martín-Lorenzo A, Hauer J, Vicente-Dueñas C, et al. Infection exposure is a causal factor in B-cell precursor acute lymphoblastic leukemia as a result of Pax5-inherited susceptibility. *Cancer Discov*. 2015;5(12): 1328-1343.
- Isidro-Hernández M, Casado-García A, Oak N, et al. Immune stress suppresses innate immune signaling in preleukemic precursor B-cells to provoke leukemia in predisposed mice. *Nat Commun*. 2023;14(1): 5159.
- Farrokhi A, Atre T, Rever J, et al. The Eμ-Ret mouse is a novel model of hyperdiploid B-cell acute lymphoblastic leukemia. *Leukemia*. 2024;38(5):969-980.
- Fidanza M, Seif AE, Demicco A, et al. Inhibition of precursor B-cell malignancy progression by toll-like receptor ligand-induced immune responses. *Leukemia*. 2016; 30(10):2116-2119.
- Davis NL, King CC, Kourtis AP. Cytomegalovirus infection in pregnancy. *Birth Defects Res*. 2017;109(5):336-346.
- Li W, Liu L, Tao R, Zheng X, Li H, Shang S. Epidemiological characteristics of human cytomegalovirus infection and glycoprotein H genotype in Chinese children. *Pediatr Neonatol*. 2020;61(1):63-67.
- Kenneson A, Cannon MJ. Review and meta-analysis of the epidemiology of congenital cytomegalovirus (CMV) infection. *Rev Med Virol*. 2007;17(4):253-276.
- Francis SS, Wallace AD, Wendt GA, et al. In utero cytomegalovirus infection and development of childhood acute lymphoblastic leukemia. *Blood*. 2017; 129(12):1680-1684.
- Wiemels JL, Wang R, Zhou M, et al. Cytomegalovirus proteins, maternal pregnancy cytokines, and their impact on neonatal immune cytokine profiles and acute lymphoblastic leukemogenesis in children. *Haematologica*. 2022;107(9):2266-2270.
- Wasserman R, Zeng XX, Hardy RR. The evolution of B precursor leukemia in the Eμ-ret mouse. *Blood*. 1998;92(1):273-282.
- Zeng XX, Zhang H, Hardy RR, Wasserman R. The fetal origin of B-precursor leukemia in the E-μ-ret mouse. *Blood*. 1998;92(10): 3529-3536.
- Duque-Afonso J, Feng J, Scherer F, et al. Comparative genomics reveals multistep pathogenesis of E2A-PBX1 acute lymphoblastic leukemia. *J Clin Invest*. 2015; 125(9):3667-3680.
- Farrell HE, Lawler C, Tan CSE, et al. Murine cytomegalovirus exploits olfaction to enter new hosts. *mBio*. 2016;7(2):e00251.
- Subramanian A, Tamayo P, Mootha VK, et al. Gene set enrichment analysis: a knowledge-based approach for interpreting genome-wide expression profiles. *Proc Natl Acad Sci U S A*. 2005;102(43):15545-15550.
- Liberzon A, Birger C, Thorvaldsdóttir H, Ghandi M, Mesirov JP, Tamayo P. The molecular signatures database (MSigDB) hallmark gene set collection. *Cell Syst*. 2015; 1(6):417-425.
- Allan JE, Shellam GR. Genetic control of murine cytomegalovirus infection: virus titres in resistant and susceptible strains of mice. *Arch Virol*. 1984;81(1-2):139-150.
- Hardy RR, Carmack CE, Shinton SA, Kemp JD, Hayakawa K. Resolution and characterization of Pro-B and Pre-Pro-B cell stages in normal mouse bone marrow. *Imaging*. 1991;173(5):1213-1225.
- Corbett NP, Blimkie D, Ho KC, et al. Ontogeny of toll-like receptor mediated cytokine responses of human blood mononuclear cells. *PLoS One*. 2010;5(11): 15041.
- Kollmann TR, Kampmann B, Mazmanian SK, Marchant A, Levy O. Protecting the newborn and young infant from infectious diseases: lessons from immune ontogeny. *Immunity*. 2017;46(3):350-363.
- Vanden Eijnden S, Goriely S, De Wit D, Goldman M, Willems F. Preferential

- production of the IL-12(p40)/IL-23(p19) heterodimer by dendritic cells from human newborns. *Eur J Immunol.* 2006;36(1):21-26.
44. Adkins B, Du R-Q. Newborn mice develop balanced Th1/Th2 primary effector responses in vivo but are biased to Th2 secondary responses. *J Immunol.* 1998;160(9):4217-4224.
  45. Mak TW, Saunders ME. T cell differentiation and effector function. In: Mak TW, Saunders ME, eds. *The Immune Response.* Academic Press; 2006:403-432.
  46. Sedger LM, Hou S, Osvath SR, et al. Bone marrow B cell apoptosis during in vivo influenza virus infection requires TNF- $\alpha$  and lymphotoxin- $\alpha$ . *J Immunol.* 2002;169(11):6193-6201.
  47. Borrow P, Hou S, Gloster S, Ashton M, Hyland L. Virus infection-associated bone marrow B cell depletion and impairment of humoral immunity to heterologous infection mediated by TNF- $\alpha$ /LT $\alpha$ . *Eur J Immunol.* 2005;35(2):524-532.
  48. Hamza T, Barnett JB, Li B. Interleukin 12 a key immunoregulatory cytokine in infection applications. *Int J Mol Sci.* 2010;11(3):789-806.
  49. Pickering H, Sen S, Arakawa-Hoyt J, et al. NK and CD8+ T cell phenotypes predict onset and control of CMV viremia after kidney transplant. *JCI Insight.* 2021;6(21):e153175.
  50. Reddehase MJ. Antigens and immunoevasins: opponents in cytomegalovirus immune surveillance. *Nat Rev Immunol.* 2002;2(11):831-844.
  51. Tsafaras GP, Ntontsi P, Xanthou G. Advantages and limitations of the neonatal immune system. *Front Pediatr.* 2020;8:5.
  52. Basha S, Surendran N, Pichichero M. Immune responses in neonates. *Expert Rev Clin Immunol.* 2014;10(9):1171-1184.
  53. Levy O. Innate immunity of the newborn: basic mechanisms and clinical correlates. *Nat Rev Immunol.* 2007;7(5):379-390.
  54. Søgaard SH, Rostgaard K, Skogstrand K, Wiemels JL, Schmiegelow K, Hjalgrim H. Neonatal inflammatory markers are associated with childhood B-cell precursor acute lymphoblastic leukemia. *Cancer Res.* 2018;78(18):5458-5463.
  55. Chang JS, Zhou M, Buffer PA, Chokkalingam AP, Metayer C, Wiemels JL. Profound deficit of IL10 at birth in children who develop childhood acute lymphoblastic leukemia. *Cancer Epidemiol Biomarkers Prev.* 2011;20(8):1736-1740.
  56. Cloppenborg T, Stanulla M, Zimmermann M, Schrappe M, Welte K, Klein C. Immunosurveillance of childhood ALL: polymorphic interferon-gamma alleles are associated with age at diagnosis and clinical risk groups. *Leukemia.* 2005;19(1):44-48.
  57. Fidanza M, Seif AE, Jo S, et al. IFN- $\gamma$  directly inhibits murine B-cell precursor leukemia-initiating cell proliferation early in life. *Eur J Immunol.* 2017;47(5):892-899.
  58. Fukao T, Frucht DM, Yap G, Gadina M, O'Shea JJ, Koyasu S. Inducible expression of Stat4 in dendritic cells and macrophages and its critical role in innate and adaptive immune responses. *J Immunol.* 2001;166(7):4446-4455.
  59. Dulson SJ, Watkins EE, Crossman DK, Harrington LE. STAT4 directs a protective innate lymphoid cell response to gastrointestinal infection. *J Immunol.* 2019;203(9):2472-2484.
  60. Deng JC, Zeng X, Newstead M, et al. STAT4 is a critical mediator of early innate immune responses against pulmonary klebsiella infection. *J Immunol.* 2004;173(6):4075-4083.
  61. Abdi K. IL-12: The role of p40 versus p75. *Scand J Immunol.* 2002;56(1):1-11.
  62. Lausten-Thomsen U, Madsen HO, Vestergaard TR, Hjalgrim H, Lando A, Schmiegelow K. Increased risk of ALL among premature infants is not explained by increased prevalence of pre-leukemic cell clones. *Blood Cells Mol Dis.* 2010;44(3):188-190.
  63. Lavoie PM, Huang Q, Jollette E, et al. Profound lack of interleukin (IL)-12/IL-23p40 in neonates born early in gestation is associated with an increased risk of sepsis. *J Infect Dis.* 2010;202(11):1754-1763.
  64. Marchant EA, Kan B, Sharma AA, et al. Attenuated innate immune defenses in very premature neonates during the neonatal period. *Pediatr Res.* 2015;78(5):492-497.
  65. Atre T, Farrokhi A, Jo S, et al. Age and ligand specificity influence the outcome of pathogen engagement on preleukemic and leukemic B-cell precursor populations. *Blood Adv.* 2023;7(22):7087-7099.
  66. Tsuzuki S, Seto M, Greaves M, Enver T. Modeling first-hit functions of the t(12;21) TEL-AML1 translocation in mice. *Proc Natl Acad Sci U S A.* 2004;101(22):8443-8448.
  67. Schindler JW, Van Buren D, Foudi A, et al. TEL-AML1 corrupts hematopoietic stem cells to persist in the bone marrow and initiate leukemia. *Cell Stem Cell.* 2009;5(1):43-53.
  68. Kasprzyk A, Harrison CJ, Secker-Walker LM. Investigation of clonal involvement of myeloid cells in Philadelphia-positive and high hyperdiploid acute lymphoblastic leukemia. *Leukemia.* 1999;13(12):2000-2006.
  69. Quijano CA, Moore D, Arthur D, Feusner J, Winter SS, Pallavicini MG. Cytogenetically aberrant cells are present in the CD34+CD33-38-19- marrow compartment in children with acute lymphoblastic leukemia. *Leukemia.* 1997;11(9):1508-1515.
  70. Greaves M. Infection, immune responses and the aetiology of childhood leukaemia. *Nat Rev Cancer.* 2006;6(3):193-203.
  71. Wiemels J. Perspectives on the causes of childhood leukemia. *Chem Biol Interact.* 2012;196(3):59-67.

© 2024 American Society of Hematology. Published by Elsevier Inc. Licensed under Creative Commons Attribution-NonCommercial-NoDerivatives 4.0 International (CC BY-NC-ND 4.0), permitting only noncommercial, nonderivative use with attribution. All other rights reserved.